(2)

Unclassified
SECURITY CLASSIFICATION OF THIS PAGE

REPORT DOCUMENTATION PAGE

1a. REPORT SECURITY CLASSIFICATION Unclassified	1b RESTRICTIVE MARKINGS None
2a. SECURITY CLASSIFICATION AUTHORITY	3 DISTRIBUTION / AVAILABILITY OF REPORT Approved for public release and sale. Distribution unlimited.
2b. DECLASSIFICATION / DOWNGRADING SCHEDULE	
4. PERFORMING ORGANIZATION REPORT NUMBER(S) ONR Technical Report No. 20	5. MONITORING ORGANIZATION REPORT NUMBER(S)
6a. NAME OF PERFORMING ORGANIZATION University of Utah 6b OFFICE SYMBOL (If applicable)	7a NAME OF MONITORING ORGANIZATION
6c. ADDRESS (City, State, and ZIP Code) Department of Chemistry Henry Eyring Building Salt Lake City, UT 84112	7b ADDRESS (City, State, and ZIP Code)
8a. NAME OF FUNDING / SPONSORING ORGANIZATION Office of Naval Research 8b OFFICE SYMBOL (If applicable)	9 PROCUREMENT INSTRUMENT IDENTIFICATION NUMBER N00014-89-J-1412
8c. ADDRESS (City, State, and ZIP Code) Chemistry Program, Code 1113 800 N. Quincy Street Arlington, VA 22217	10 SOURCE OF FUNDING NUMBERS PROGRAM ELEMENT NO. / PROJECT NO. / TASK NO. / WORK UNIT ACCESSION NO

11. TITLE (Include Security Classification)
Identification of Tetragonal and Cubic Structures of Zirconia

12. PERSONAL AUTHOR(S) R. Srinivasan, R. J. DeAngelis, G. Ice, S. F. Simpson, J. M. Harris, B. H. Davis

13a TYPE OF REPORT	13b. TIME COVERED	14. DATE OF REPORT (Year, Month, Day)	15. PAGE COUNT
Technical	FROM 6/89 TO 5/90	May 29, 1990	37

16. SUPPLEMENTARY NOTATION

17 COSATI CODES			18. SUBJECT TERMS (Continue on reverse if necessary and identify by block number)
FIELD	GROUP	SUB-GROUP	Raman spectroscopy of ceramic structures; cubic and tetragonal crystal structures of zirconia

19. ABSTRACT (Continue on reverse if necessary and identify by block number)

Attached.

20 DISTRIBUTION / AVAILABILITY OF ABSTRACT ☒ UNCLASSIFIED/UNLIMITED ☐ SAME AS RPT ☐ DTIC USERS	21 ABSTRACT SECURITY CLASSIFICATION Unclassified
22a NAME OF RESPONSIBLE INDIVIDUAL Joel M. Harris	22b TELEPHONE (Include Area Code) (801)581-3585 22c OFFICE SYMBOL

DD FORM 1473, 84 MAR 83 APR edition may be used until exhausted
All other editions are obsolete.

SECURITY CLASSIFICATION OF THIS PAGE
Unclassified

OFFICE OF NAVAL RESEARCH

Grant No: N00014-89-J-1412

R&T Code 413a005---03

Technical Report No. 20

Identification of Tetragonal and Cubic Structures of Zirconia

Prepared for publication in Journal of Materials Research

by

R. Srinivasan, R. J. DeAngelis, G. Ice, S. F. Simpson, J. M. Harris, and B. H. Davis

Department of Chemistry
University of Utah
Salt Lake City, UT 84112

Department of Material Science and Center for Applied Energy Research
University of Kentucky
Lexington, KY 40506

Oak Ridge National Laboratory
Oak Ridge, TN 37831

May 29, 1990

IDENTIFICATION OF TETRAGONAL AND CUBIC STRUCTURES OF ZIRCONIA

Ram Srinivasan,[1,2] Robert J. De Angelis,[1], Gene Ice,[3]

Stanley F. Simpson,[4] Joel M. Harris,[4] and Burtron H. Davis[1,2]

1. Department of Materials Science and Engineering

University of Kentucky

Lexington, KY 40506-0046

2. Center for Applied Energy Research

University of Kentucky

3572 Iron Works Pike

Lexington, KY 40511-8433

3. Oak Ridge National Laboratory

Oak Ridge, TN 37831

4. Department of Chemistry

University of Utah

Salt Lake City, UT 84112

ABSTRACT

X-ray diffraction from a synchrotron source was employed in an attempt to identify definitively the crystal structures in zirconia ceramics produced by sol-gel method. The particles of chemically precipitated zirconia, after calcination below 600°C, are very fine, and have a diffracting particle size in the range of 7-15 nm. Since the tetragonal and cubic structures of zirconia have very similar lattice parameters, it is difficult to distinguish between the two. The tetragonal structure can be identified only by the characteristic splittings of the Bragg profiles from the "c" index planes. However, these split Bragg peaks from the tetragonal phase in zirconia overlap with one another due to particle size broadening. In order to distinguish between the tetragonal and cubic structures of zirconia, three samples were studied using synchrotron radiation. The results indicated that a sample containing 13 mol.% yttria-stabilized zirconia possessed the cubic structure with a_o = 0.51420 $\pm$ 0.00012 nm. A sample containing 6.5 mol.% yttria stabilized zirconia was found to consist of a mixture of cubic and tetragonal phases with the cubic phase being the major constituent, with a_o = 0.51430 $\pm$ 0.00008 nm. Finally, a sample which was precipitated from a pH 13.5 solution was observed to have the tetragonal structure with a_o = 0.51441 $\pm$ 0.00085 nm and c_o = 0.51902 $\pm$ 0.00086. Raman studies on these samples corroborate the X-ray diffraction results. The X-ray diffraction data obtained from a synchrotron source are superior to the data obtained

by conventional X-ray diffraction sources in identifying the crystal structures of very fine crystalline materials.

INTRODUCTION

Zirconia is a polymorphic ceramic which may exist in three well-known structural forms: monoclinic, tetragonal, and cubic[1-6]. Recently, a high-pressure allotropic form of zirconia (orthorhombic) has been reported; this phase is metastable at atmospheric pressure and reverts to the monoclinic form by such a mild treatment as grinding in a mortar[7]. Although a tremendous amount of research has been carried out to elucidate the crystal structures of industrially important zirconia ceramics, problems remain in assigning the structures accurately. Garvie et al.[8] reported a cubic dispersion in the tetragonal structure; this appears to have been the only observation of this material. Mazdiyasni et al.[9] reported that a cubic phase could be obtained by the addition of 6.5 mol.% yttria, following an alkoxide preparation route.

It has been observed that although the monoclinic phase is stable below 1100°C, the tetragonal phase may, under certain conditions, be stabilized at lower temperatures[10]. Several explanations for the low-temperature stabilization of the tetragonal phase have been postulated[11-16]. Garvie[10-12] proposed that the low-temperature tetragonal phase stability is due to the lower surface energy of the tetragonal phase relative to that of the monoclinic phase. It has been suggested that small amounts (about 0.75 wt.%) of bound OH groups in solid solution stabilize the

tetragonal structure at room temperature[13]. Others[14,15] have reported that the presence of water vapor catalyzes the t → m transformation in zirconia, and in this way determines which phase is observed. It has also been postulated that structural similarities between the precursor gels and the tetragonal structure are responsible for the low-temperature stabilization of the tetragonal phase in zirconia[17]. Clearfield[18] recently offered an explanation to account for the formation of tetragonal or monoclinic; here he proposes precipitation following two pathways, one leading to tetragonal and one to monoclinic zirconia following calcination. As is apparent from the many conflicting studies, the actual mechanism for the low-temperature stabilization of tetragonal phase of zirconia remains obscure.

Mitsuhashi et al.[19] prepared amorphous zirconia from $ZrOCl_2 \cdot 8H_2O$ with ammonia and obtained pure tetragonal zirconia upon heating the product. It was reported that fine single-domain tetragonal particles, which are strain-free, are more easily transformed than the poly-domain particles. However, Mitsuhashi et al.[19] did not specify the pH of the precipitation.

Katz[20] reported that a metastable cubic phase results from the precipitation of $ZrOCl_2$ with NaOH, again without specifying the pH of the precipitation.

Davis[21] found that the pH at which the precursor gels are precipitated causes the tetragonal or the monoclinic phase to be formed after calcining the material at 400 - 600°C. It was reported that the tetragonal phase could be obtained either at a low pH (3-5) range or at a high pH range (13-14), and that the monoclinic phase

could be obtained in the medium pH (8-11) range. Srinivasan et al.[22] demonstrated that the tetragonal phase obtained at pH 13.5 was stable even after calcination at 500°C for 300 hours and later found that both the monoclinic and tetragonal phases could be obtained at a pH of 10.5, depending upon the time taken to effect the precipitation[23]. Most recently, Jada and Peletis[24] suggested that the solution chemistry of zirconia precursor materials plays a key role in controlling the formation of the crystal structure, polymorphic transformation, and crystalline growth. Mamott et al.[25] using a time-resolved dynamic high-temperature XRPD (X-ray Powder Diffraction) technique, have reported on the onset of an ordering within the amorphous starting material, and on the progress of its conversion into crystalline zirconia.

The assignment of cubic and tetragonal structures, based solely on the X-ray diffraction analysis, can be misleading because the cubic and tetragonal structures (a_o = 0.5124 nm for cubic, and a_o = 0.5094 nm and c_o = 0.5177 nm for tetragonal structures) are very similar[26]. Srivastava et al.[27] reported that the tetragonal structure can be distinguished from the cubic structure by the presence of the characteristic splittings of the tetragonal phase, such as (002) (200), (113) (311), (004) (400) and (006) (600) etc., whereas the cubic phase exhibits only single peaks at all of these positions. Garvie et al.[8] utilized high-angle reflections to distinguish the cubic and tetragonal structures and to determine their relative proportions. In an investigation of plasma-sprayed yttria-stabilized zirconia coatings, Miller et al.[28,29] used the (400)

region of the X-ray diffraction patterns in order to calculate the relative proportions of cubic and tetragonal phases. They reported that the dominant peaks in this region change from the monoclinic to tetragonal and gradually to the cubic reflections with an increase in the level of yttria. A "curve resolver" was used to separate the tetragonal and cubic peak compon.s in the (400) region[29] and the 'd' values for the (400) and (004) tetragonal peaks were calculated from the curve-resolved peak positions.

It should also be noted that in order to clearly observe the tetragonal splittings in the entire 2θ region in yttria-containing zirconia ceramics, the material must be sintered above 1100°C. Below 1100°C, the 2θ angle at which tetragonal reflections occur becomes a function of a number of parameters, such as the change in composition, different thermal treatments, variation of the lattice parameters with change in composition, etc. Hannink[30] has commented that the $(400)_c$ profile could not be resolved from the $(400)_t$ and $(004)_t$ reflections in diffractometer traces such that relative amounts of each phase could be determined. Paterson et al.[31] reported the presence of the t' phase, that is strongly related to the cubic phase, and this t' phase was observed in the 2θ region 72-76°.

As these aforementioned works suggest, the 2θ region used in the assignment and calculation of tetragonal and cubic phases in ZrO_2 is complex; care must be exercised when evaluating these crystalline phases using XRD data alone. For samples prepared by precipitation, the doublets of the tetragonal phase at

intermediate 2θ positions are difficult to distinguish clearly because of the peak broadening due to the small crystallite size. Davis[21] and Srinivasan et al.[22,23] have suggested that the crystal structure obtained at low pH values and high pH ranges is the tetragonal structure, although the tetragonal doublets are not readily apparent in XRD. To confirm their crystal assignment, Davis[21] and Srinivasan et al.[22,23] utilized Raman spectroscopy. In contrast to XRD, the monoclinic, tetragonal, and cubic zirconia structures can be readily distinguished from one another by Raman spectroscopy. Various experimental[32,33] and group theoretical calculations[34] reveal that the Raman spectrum for the monoclinic phase should contain 18 bands, the tetragonal phase spectrum 5 bands, and the cubic phase should possess only one band. Recently, we assigned a tetragonal structure to a zirconia material precipitated from a solution of pH 13.5. This assignment was based upon both XRD and Raman spectral evidence that was in agreement with previously published spectroscopic data for the crystalline phases. However, Benedetti et al.[35] have recently reassigned a cubic structure to a zirconia sample prepared in a similar manner. In this paper, we report further XRD results obtained using a synchrotron source and Raman data which support our previous assignment in yet another attempt to further the understanding of the crystal structures in precipitated zirconia ceramic materials.

EXPERIMENTAL

The complete listing of the specifications for all of the zirconia samples used in this study are presented in Table 1. The 13 mole% yttria-stabilized zirconia labeled

as sample A was prepared from yttrium and zirconium nitrates using a coprecipitation technique and dried at 120°C. Sample B was prepared in a manner similar to Mazdiyasni et al.[9] and contained 6.5 mole% yttria. Both samples A and B were calcined at 1150°C for 10 hours. Zirconia sample C was precipitated from a solution of 0.3 M $ZrCl_4$ that was adjusted to pH 13.5 with KOH. The resulting product was washed to a negative test for chloride ion (ca. 10 washings) and then calcined at 500°C for 200 hours[22,23].

Samples D and E were prepared in a manner similar to that reported by Benedetti et al.[35]. Sample D, which corresponds to Sample III in reference 35, was washed twice while Sample E (Sample II in reference 35) was washed exhaustively. Subsequent atomic absorption analysis demonstrated that sample D contained ca. 3 wt.% Na and that sample E contained less than 0.5 wt.% Na.

The Raman system used to acquire the spectroscopic data consisted of a Coherent INNOVA 90 krypton ion laser source, a triple monochromator (Model 1877, Spex Industries), and a charge-coupled-device detector (Model CSF THF7882CDA, Thomson). Spectra were collected using a 10 minute counting time and ca. 5 mW illumination power at the sample. Following data collection, data were transferred to a micrcomputer for subsequent analysis and plotting.

Much of the XRD data reported here were obtained using a synchrotron source. The experiments for our samples were conducted on the beam line X14 (Oak Ridge National Laboratory) at the National Synchrotron Light Source at

Brookhaven National Laboratory, Upton, New York. The experiments were performed at room temperature without a single crystal monochromator in the diffraction beam path. Diffraction data were collected by step scanning for times of one or two seconds per step and a step width of 0.02 or 0.01 degrees in 2θ. One of the primary objectives of this investigation was to obtain diffraction data using a synchrotron source that would allow us to clearly distinguish between the tetragonal and cubic structures in zirconia.

RESULTS AND DISCUSSION

Synchrotron radiation is a powerful tool for diffraction studies. In structural areas, it provides the ability to measure scattering curves to very large values of K ($= \mathrm{Sin}\theta/\lambda$)[36]. The high intensity and collimation of synchrotron radiation allows high resolution studies, both in the small and high angle regions, and also very close to Bragg reflections. This is useful in a number of applications, including structure analysis[37].

A typical X-ray pattern collected on the synchrotron beam line from a sample of pure monoclinic (> 95%) zirconia is presented in Figure 1A. This material was prepared from a batch of zirconyl nitrate hydrate; another batch of zirconyl nitrate hydrate from this same supplier produced a material containing a high percentage of tetragonal zirconia. We have been able to obtain this high percentage of monoclinic form by precipitation at pH 10 only when the initial zirconium species is well dispersed, presumably as a monoatomic zirconium species. In most cases, zirconyl

salts appear to be polymeric dispersions and this invariably leads to a high percentage of tetragonal zirconia.

The importance of the starting zirconium salt has been ignored repeatedly by workers in the preparation of crystalline zirconia ceramics by precipitation, and we feel that this is a likely source for the diversity of results that have been reported.

ttern for the tetragonal form of zirconia is shown in Figure 1B. It is obvious that the XRD pattern clearly distinguishes the tetragonal and cubic structures from the monoclinic form. However, the XRD patterns for (111) reflections of the cubic 13 wt.% yttria-stabilized zirconia (Figure 1C) and tetragonal zirconia (Figure 1B) are essentially coincident, and therefore the two cannot be distinguished readily from the XRD patterns. Thus, other means of distinguishing between tetragonal and cubic forms becomes necessary.

The 2θ region containing the (002) and (200) profiles of tetragonal zirconia for Samples A, B, and C is shown in Figure 2. The (200) cubic profile of Sample A is evident with a calculated crystallite size of about 103 nm using the Scherrer equation[38]. This profile is very broad for Sample B and indicates a crystallite size of 10.2 nm. Although the doublets cannot be seen clearly in Sample C, the asymmetry of the peak indicates an overlap of tetragonal doublets. Because of particle size broadening, the (002) and (200) profiles are unresolved and appear as one broad peak (Figure 2C). The calculated size is ca. 10 nm for Sample C; this assumes only one peak is present.

Another 2θ region of interest is 48-53°, where the (220) and (202) tetragonal peaks should appear as a doublet, and the cubic (220) peak should appear as a single peak. This region is shown in Figure 3, wherein the (220) cubic peak is observed for Sample A, and a broad peak for Sample B. For the pH 13.5 material, the tetragonal doublets are not well resolved. (This is further evidence for tetragonal doublets that overlap due to particle size broadening.) The crystallite size for Sample C, measured from the full width at half maximum intensity[38] is 10.3 nm, and the crystallite size for Sample B is 9.5 nm. The measured crystallite size for Sample A is 105. nm, which is nearly ten times larger than the Samples B and C. The 2θ region covering the (113) and (311) tetragonal doublets for the three samples is shown in Figure 4. For the pH 13.5 material (Sample C), the tetragonal doublets begin to appear as indicated by the peak asymmetry, whereas the 13 mol.% yttria stabilized zirconia (Sample A) shows only the (311) cubic peak. As can be seen, the particle size broadening certainly increases the difficulty in the assignment of the tetragonal doublets.

The 2θ region containing (004) and (400) tetragonal doublets is presented in Figure 5 for all the three samples, and this region was plotted exclusively for Sample C in Figure 6. This 2θ region has been extensively used by researchers in order to distinguish the cubic from the tetragonal structure in zirconia[8,28,35,39]. For Sample A the (400) cubic peak is very sharp with a calculated crystallite size of about 96 nm. For Sample B (6 mol.% yttria stabilized zirconia) the profile is very broad and

appears to be a mixture of tetragonal and cubic phases with a crystallite size estimation of 8.5 nm. However, for Sample C (Figures 5c and 6), the (004) and (400) tetragonal doublets can be observed clearly.

The 2θ region from 79-86° (Figure 7) shows the (331) and (420) cubic peaks for Sample A. The tetragonal doublets (331) and (313) and (420) and (402) are not well resolved for Sample C. The high angle region from 120-134° is plotted in Figure 8. Here the (600) cubic peak is observed for Sample A; for Sample C (006) and (600) tetragonal doublets are observed.

Both the conventional X-ray source and synchrotron source were used to obtain patterns from samples B and C and these contained broad diffraction lines. This indicates the very small crystallite size of the chemically precipitated materials. Despite the broad diffraction lines, a complete XRD pattern was obtained for all the three samples so as to offer a reasonable definition of the crystal structures developed in these materials. Based on the above XRD results, the crystallite size data were calculated using Scherrer analysis[38], and these data are presented in Table 2.

The results obtained from Raman spectroscopy are shown in Figures 9 and 10. The spectrum from Sample A (Figure 9A) shows the characteristic Raman band for a cubic zirconia at 625 cm^{-1}. The spectrum from Sample D (Figure 9D) exhibits the characteristic Raman bands of tetragonal zirconia. We have obtained similar spectra for a number of samples that we have prepared at pH values in the 13-14

range[23]. We experieced consistent difficulties in obtaining a complete Raman spectrum for Sample B.

Raman spectra (Figure 10) were obtained from the two samples that were prepared in like manner to Samples II and III of Reference 35. Sample D was washed only two times and was found to contain about 3 wt.% Na while Sample E was washed thoroughly and contained less than 0.5 wt.% Na. Samples D and E exhibit Raman spectra whose peak positions agree with those expected for the tetragonal form[32]. However, the XRD for sample D does not show the anticipated two distinct peaks at about $2\theta = 35°$. Due to peak broadening, we are unable to confirm the tetragonal form by the presence of the (002) diffraction line splitting at $2\theta = 35°$. Also shown in Figure 10 is the Raman spectrum for the more completely washed material that was precipitated at pH 13.5 (Figure 10E, corresponding to Sample II, reference 35). This sample likewise displays a spectrum with band positions which indicate the tetragonal form. The band positions for both the minimally washed and thoroughly washed materials (spectra presented in Figure 10) are consistent with the tetragonal form although the spectra are of a poorer quality.

The literature for zirconia has inconsistencies, both with regard to structure and to lattice parameters. It is known that the stabilization of zirconia with 13 mol.% or 6 mol.% yttria will alter the lattice parameters, and we have considered these two samples only for comparative studies with a tetragonal zirconia precipitated at a pH of 13.5 (Sample C). The lattice parameters calculated from the diffraction data using

a least-square fit[40], indicate that Sample A has a cubic structure with a_o = 0.51420 ± 0.00012 nm. This conclusion is further substantiated by the Raman spectrum of sample A. Likewise, Sample C is undoubtedly tetragonal zirconia.

We feel that the statement of Benedetti et al.[35] that the pH 13.5 material, if washed minimally, is cubic (a_o = 0.5116 nm), is questionable. The X-ray diffraction patterns from sample D (washed only 2 times) are presented in Figure 11. Although the $(004)_t$ and $(400)_t$ phases are not resolved well in the 2θ region of 70-78°, the $(006)_t$ and $(600)_t$ phases are well resolved in the 2θ range of 120-132°. Calling this peak 'cubic', based on the inability to observe the $(004)_t$ and $(400)_t$, will be misleading without checking carefully at the higher angle peaks [i.e. $(006)_t$ and $(600)_t$]. One must therefore exercise extreme caution in assigning a structure to the pH 13.5 material. One cannot assign either the tetragonal or the cubic structure relying solely on the 2θ range of 70-76°, a region which contains only the (004) and (400) tetragonal doublets and the (400) cubic singlet. As a result of the ambiguity surrounding the true crystal structure of the pH 13.5 material, we have undertaken XRD studies using a synchrotron source. With conventional X-ray diffraction, because of the very small crystallite size, the tetragonal doublets often cannot be clearly resolved. On the other hand, XRD studies utilizing a synchrotron source have the capability of distinguishing further the tetragonal doublets even for a material consisting of very fine crystallites. Hence, one should examine higher order peaks, such as (006) and (600) tetragonal doublets in the 2θ range of 120-132°, to ascertain

accurately the crystal identity. In order to corroborate this conclusion further, we recommend that Raman studies also be undertaken. The Raman spectrum for tetragonal zirconia in Figures 9 and 10 lends support to our conclusion that the pH 13.5 material is tetragonal. For zirconia precipitated employing NaOH to produce pH 13.5, the tetragonal form has been obtained whether the washing was limited or extensive. We have not obtained evidence to support the view that ca. 3% Na can stabilize the cubic form of zirconia as was reported in Reference 35.

CONCLUSIONS

X-ray diffraction using a high-intensity synchrotron source has been adopted to provide a better definition of certain controversial points in the assignment of the crystal structure in zirconia. It is clear that if zirconia is precipitated at a pH of 13.5, it develops the tetragonal phase and not the cubic form. Both Raman and XRD studies lend support to our conclusions about the developed structure in the precipitated zirconia. We have found that particle size broadening of XRD profiles can lead potentially to incorrect structural assignments. It is therefore concluded that a more complete analysis including Raman spectroscopy in addition to XRD should be undertaken before positively assigning the crystal structures to materials of very small crystallite size, a situation in which particle size broadening of XRD data can be overwhelming.

ACKNOWLEDGMENTS

This work was supported, in part, by the Commonwealth of Kentucky through the University of Kentucky, Center for Applied Energy Research Laboratory, the Department of Energy, Contract No. DE-FG05-85ER45186 at the University of Kentucky, and by a grant from the Office of Naval Research at the University of Utah. Travel grants from the Oak Ridge Associated Universities, ORNL, Tennessee, to undertake the trip to the Brookhaven National Laboratory are gratefully acknowledged.

REFERENCES

1. O. Ruff and F. Z. Ebert, Anorg. U. All. Gem. Chem., 180, 19-41 (1929).
2. P. Murray and E. B. Allison, Trans. Brit. Ceram. Soc., 53 [6], 335-61 (1954).
3. C. T. Lynch, F. W. Bahldiek and L. B. Robinson, J. Am. Ceram. Soc., 44 [3], 147-48 (1961).
4. R. N. Patil and E. C. Subba Rao, Acta Crystallog., A26, 555 (1970).
5. H. S. Maiti, K. V. G. K. Gokhale and E. C. Subba Rao, J. Am. Ceram. Soc., 55 [6], 317-22 (1972).
6. A. H. Hueur and M. Rühle in "Advances in Ceramics", Vol. 12, N. Claussen, M. Rühle and A. H. Hueur, eds., Am. Ceram. Soc., Columbus, OH, 1984, pp 1-13.
7. R. Suyama, T. Ashida and S. Kume, J. Am. Ceram. Soc., 68 [12] C-134 (1985).
8. R. C. Garvie, R. H. Hannink and R. T. Pascoe, Nature, 258, 703 (1975).
9. K. S. Mazdiyasni, C. T. Lynch and J. S. Smith, II, J. Am. Ceram. Soc., 50 [10], 532 (1967).
10. R. C. Garvie, J. Phys. Chem., 69, 1238 (1965).
11. R. C. Garvie, J. Phys. Chem.,82, 218 (1985).
12. R. C. Garvie and M. V. Swain, J. Mater. Sci., 20, 1193 (1985).
13. R. Cyprês, R. Wollast and J. Raucq, Ber. Deut. Keram. Ges., 40, 527 (1963).
14. Y. Murase and E. Kato, J. Am. Ceram. Soc., 66 [3], 196 (1983).
15. Y. Murase and E. Kato, J. Am. Ceram. Soc., 62 [9-10], 527 (1979).

16. P. E. D. Morgan, J. Am. Ceram. Soc., 67 [10], C-204 (1984).

17. J. Livage, K. Doi and J. Maziers, J. Am. Ceram. Soc., 51, 349 (1968).

18. A. Clearfield, J. Mater. Res., 5, 161-2 (1990).

19. J. Mitsuhashi, M. Ichihara and U. [illegible] Am. Ceram. Soc., 57 [2], 97-101 (1974).

20. G. Katz, J. Am. Ceram. Soc., Discussions and Notes, 54 [10], 531 (1971).

21. [illegible] H. Davis, J. Am. Ceram. Soc., 67 [8], C-168 (1984).

22. R. Srinivasan, R. J. De Angelis and B. H. Davis, J. Mater. Res., 1, 538 (1987).

23. R. Srinivasan. M. B. Harris, S. F. Simpson, R. J. De Angelis and B. H. Davis, J. Mater. Res., 3 [4], 787 (1988).

24. S. S. Jada and N. G. Peletis, J. Mater. Sci. Lett., 8, 243-246 (1989).

25. G. T. Mamott, P. Barnes, S. E. Tarling, S. L. Jones and C. J. Norman, Powder Diffraction., 3 [4], 234-239 (1988).

26. Magnesium Elektron Publication #113, "Zirconia and Zirconia Ceramics", R. Stevens, ed., published by Magnesium Elektron Ltd., 1986.

27. K. K. Srivastava, R. N. Patil, C. B. Choudhary, K. V. G. K. Gokhale and E. C. Subba Rao, Trans. Brit. Ceram. Soc., 73 [5], 85-91 (1974).

28. R. A. Miller, R. G. Garlick and J. L. Smialek, J. Am. Ceram. Soc. Bull., 62 [12], (1983).

29. R. A. Miller, J. L. Smialek and R. G. Garlick in Adv. Ceram. III. Science and Technology of Zirconia, A. H. Hener and L. W. Hobbs, eds., Am. Ceram. Soc., Columbus, OH, 1981, pp 241-253.

30. R. H. J. Hannink, J. Mater. Sci., 13, 2487 (1978).

31. A. Paterson and R. Stevens, J. Mater. Res., 1 [2], 295 (1986).

32. C. M. Phillippi and K. S. Mazdiyasni, J. Am. Ceram. Soc., 54 [5] 254 (1971).

33. V. G. Kermidas and W. B. White, J. Am. Ceram. Soc., 57 [1], 22 (1974).

34. W. B. White, Mater. Res. Bull., 2 [3], 381 (1967).

35. A. Benedetti, G. Fagherazzi and F. Pinna, J. Am. Ceram. Soc., 72 [3], 467 (1989).

36. Final report on the Workshop on the Applications of Synchrotron Radiation to X-ray Diffraction Problems in Materials Science, Cornell University, Ithaca, NY, 14853.

37. J. B. Hastings, W. Thomlinson and D. E. Cox., J. Appl. Cryst., 17, 85-89 (1984).

38. H. P. Klug and L. E. Alexander, "X-ray Diffraction Procedures", Wiley, New York, (1967) 491.

39. T. K. Gupta, J. Mater. Sci., 12, 2421-2426 (1977).

40. M. H. Mueller, L. Heaton and K. T. Miller, Acta Crystallogr., 13, 828 (1960).

FIGURE LEGEND

Figure 1. Typical X-ray diffraction patterns using a synchrotron source. (A) 100% monoclinic zirconia precipitated at pH 10.5 and calcined at 500°C - 5h, (B) 100% tetragonal zirconia (Sample C) and (C) 100% cubic zirconia (Sample A).

Figure 2. X-ray diffraction patterns in the 2θ region of 33-37°, in which the (200) cubic and (200) (002) tetragonal doublets occur. (A) Sample A, (B) Sample B, and (C) Sample C.

Figure 3. X-ray diffraction patterns for Samples A, B, and C in the 2θ region of 48-53°. In this region the (220) cubic peak is evident for Sample A (Curve A). The (202) and (220) tetragonal doublets can be seen overlapping, because of particle size broadening (Curve C).

Figure 4. X-ray diffraction patterns for Samples A, B, and C in the 2θ region of 58-61°. Curve (A) shows the (311) cubic profile for Sample A. Curve B shows a broad (311) cubic phase, and Curve C corresponds to Sample C. (The pattern for Sample C is broadened by the tetragonal doublets (113) and (311) peaks.)

Figure 5. X-ray diffraction pattern for Samples A, B, and C in the 2θ region of 71-76°, where the (400) cubic peak and (004) (400) tetragonal doublets should appear. Curves (A), (B), and (C) refer to Samples A, B, and C, respectively.

Figure 6. X-ray diffraction pattern for Sample C, where (004) and (400) tetragonal doublets can be seen clearly resolved.

Figure 7. X-ray diffraction patterns for Samples A, B, and C, in the 2θ region of 79-86°. The (331) and (420) cubic peaks are evident for Sample A (Curve A). These two peaks are broadened in Sample B (Curve B). The tetragonal doublets (331) (313) and (420) (402) are not well-resolved for Sample C (Curve C).

Figure 8. X-ray diffraction patterns for Samples A and C in the 2θ region of 120-134°. Sample A shows (531) and (600) cubic peaks. Sample C shows the overlapping (513) and (531) tetragonal doublets. The (006) and (600) tetragonal doublet can be observed clearly without overlap.

Figure 9. Raman spectra obtained for Samples A and D. Sample A has the cubic structure as indicated by the characteristic Raman band at 625 cm^{-1}. Sample D (the feebly washed pH 13.5 material) stands in absolute contrast with the cubic structure.

Figure 10. Raman spectra for Samples D and E. The characteristic Raman bands at 262, 330, 473, 613 and 643 cm^{-1}, suggest that the material is tetragonal. The relative band positions for D and E indicate that both samples possess the tetragonal structures.

Figure 11. X-ray diffraction patterns for Sample D. Although the $(004)_t$ and $(400)_t$ are not well resolved, the $(006)_t$ and $(600)_t$ profiles can be seen clearly resolved.

Table 1

Descriptions of the Specimens

Sample ID	Specifications
Sample A	13 mol.% yttria-stabilized ZrO_2 - calcined at 1150°C - 10 h.
Sample B	7.5 mol.% yttria-stabilized ZrO_2 obtained from Ref. 9 - calcined at 1150°C - 10 h.
Sample C	ZrO_2 precipitated at pH 13.5 - calcined at 500°C for 200 hours.
Sample D	ZrO_2 precipitated using 4M NaOH at pH 14.0 - gels were washed two times only - containing about 3 wt.% Na.
Sample E	ZrO_2 precipitated using 4M NaOH at pH 14.0 - gels thoroughly washed - containing < 0.5 wt.% Na.

Table 2

Crystallite Size Data for Samples A, B and C

	Crystallite Size (nm)													
	(111)	(200)	(002)	(220)	(202)	(311)	(113)	(222)	(400)	(004)	(331)	(420)	(600)	(006)
Sample A	106	103	---	105.5	---	102	---	91	96	---	101	104	95	---
Sample B	10	10.2	10.2	9.5	9.5	9.5	9.5	9	8.5	8.5	9.5	9.2	*	*
Sample C	13	9	9	10.3	10.3	8	8	11.2	10.8	8.5	9.5	7.5	5	5.2

* Not available.

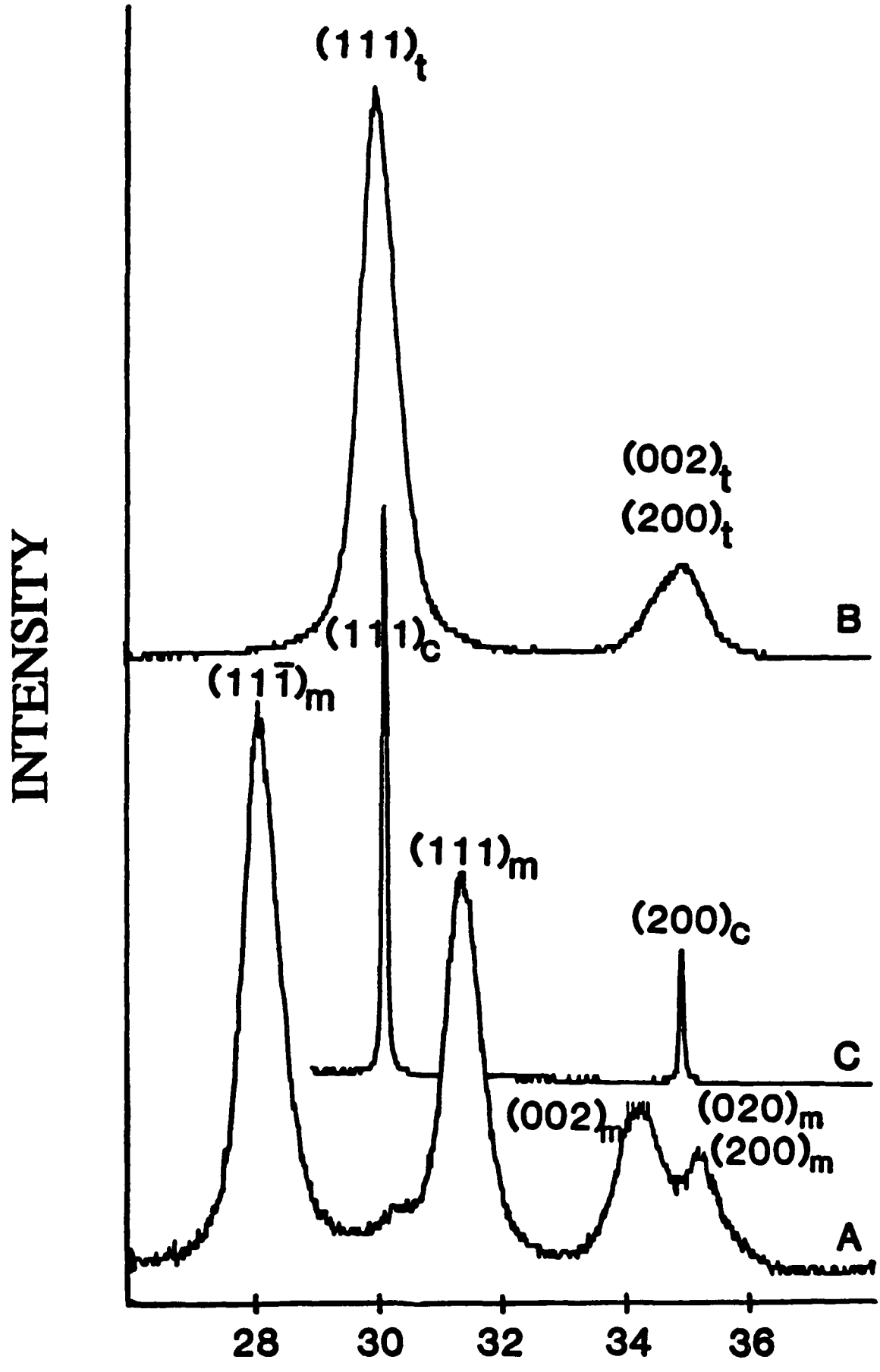
(111)t
(002)t
(200)t
B
(111)c
(11$\bar{1}$)m
(111)m
(200)c
C
(002)m
(020)m
(200)m
A
INTENSITY
28
30
32
34
36
2θ

Fig 1

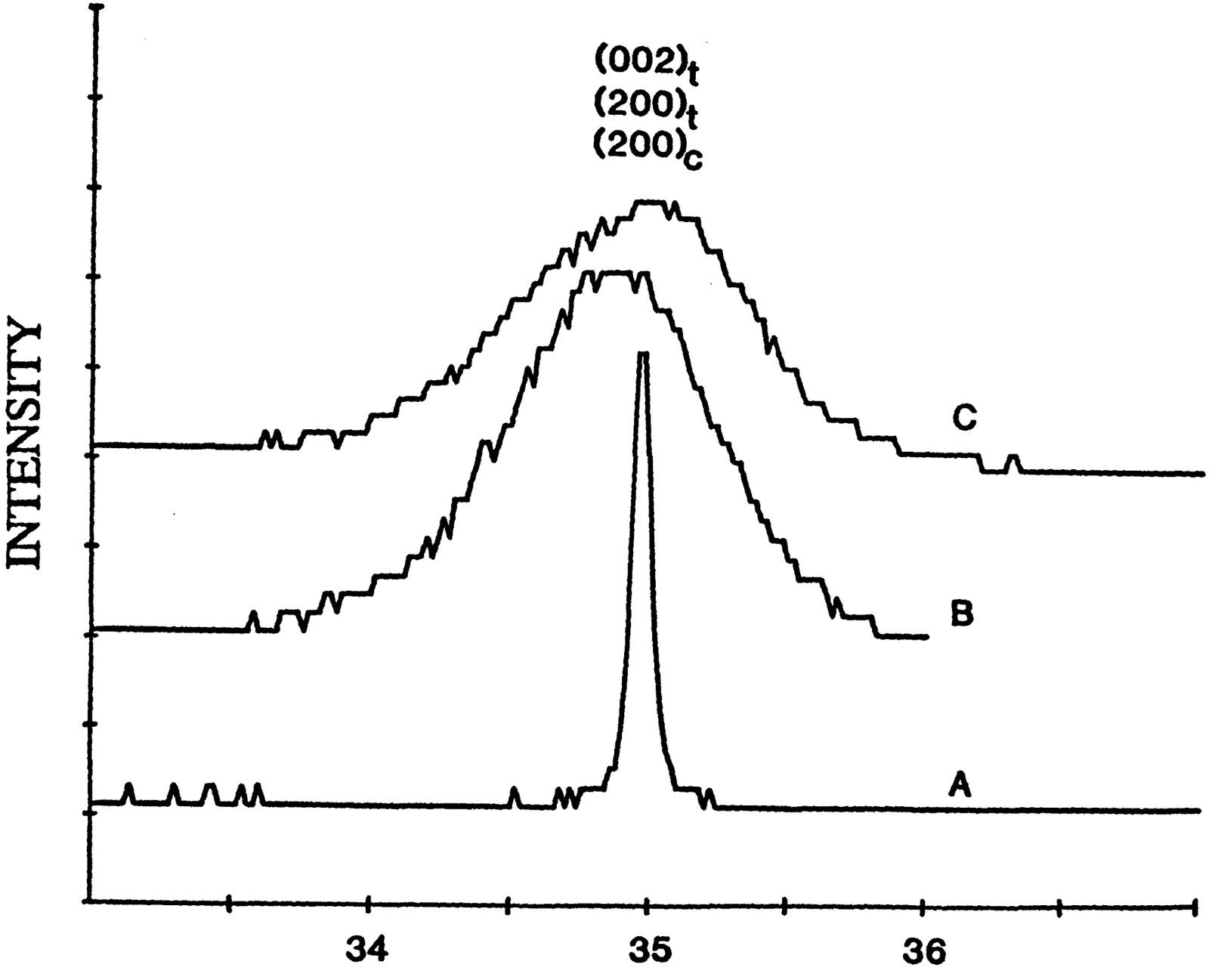

Fig 2

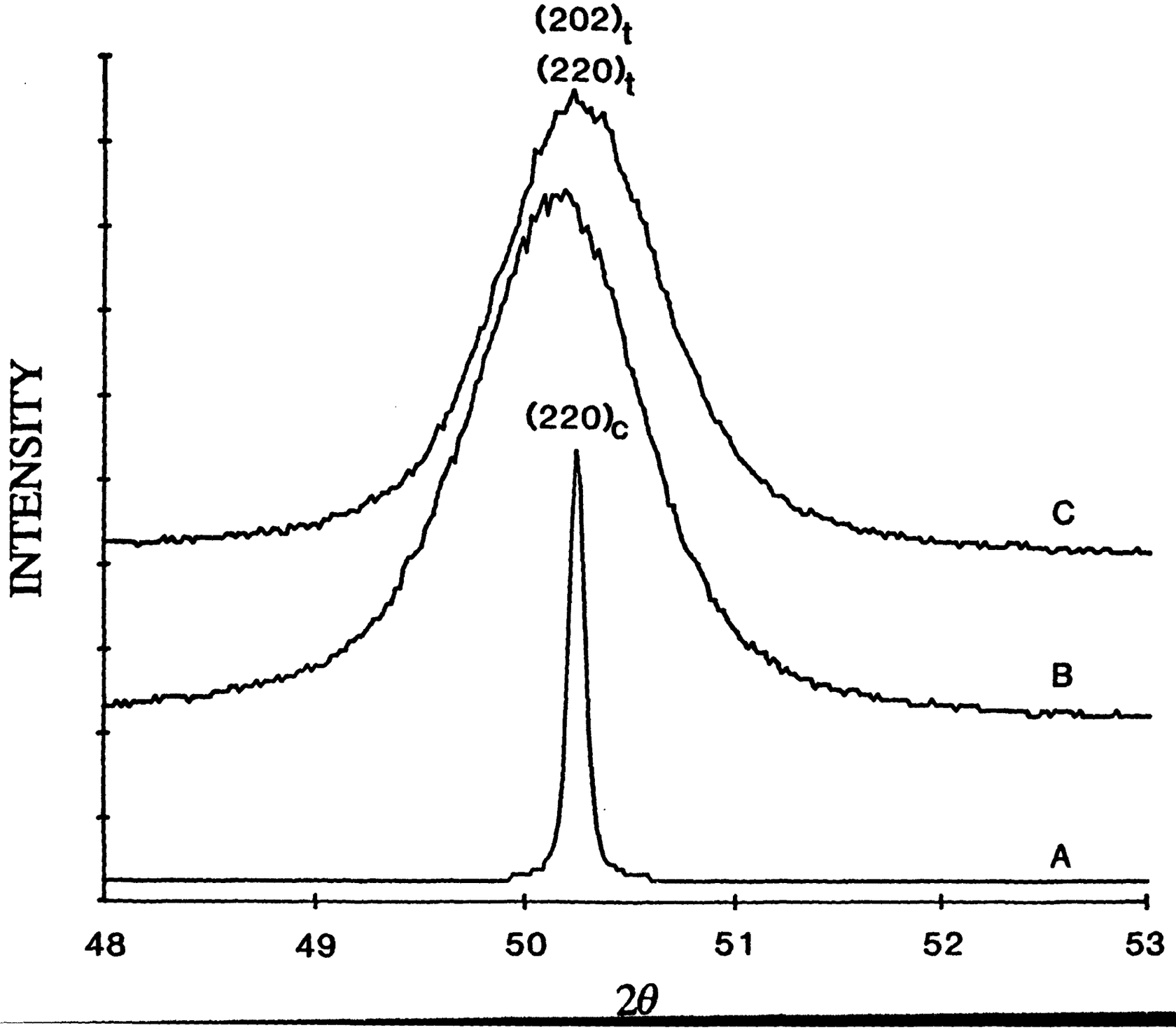

Fig 3

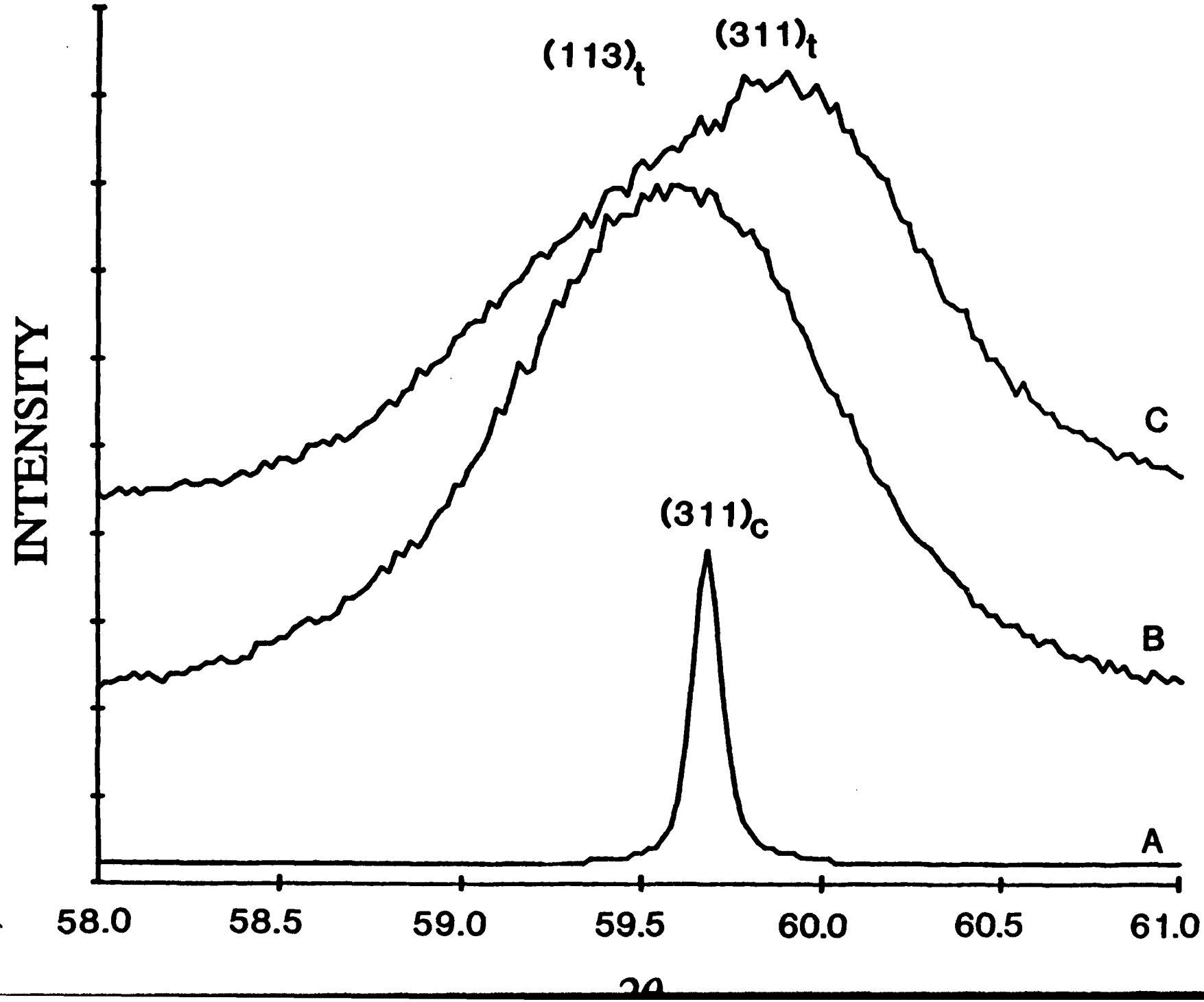

Fig 4

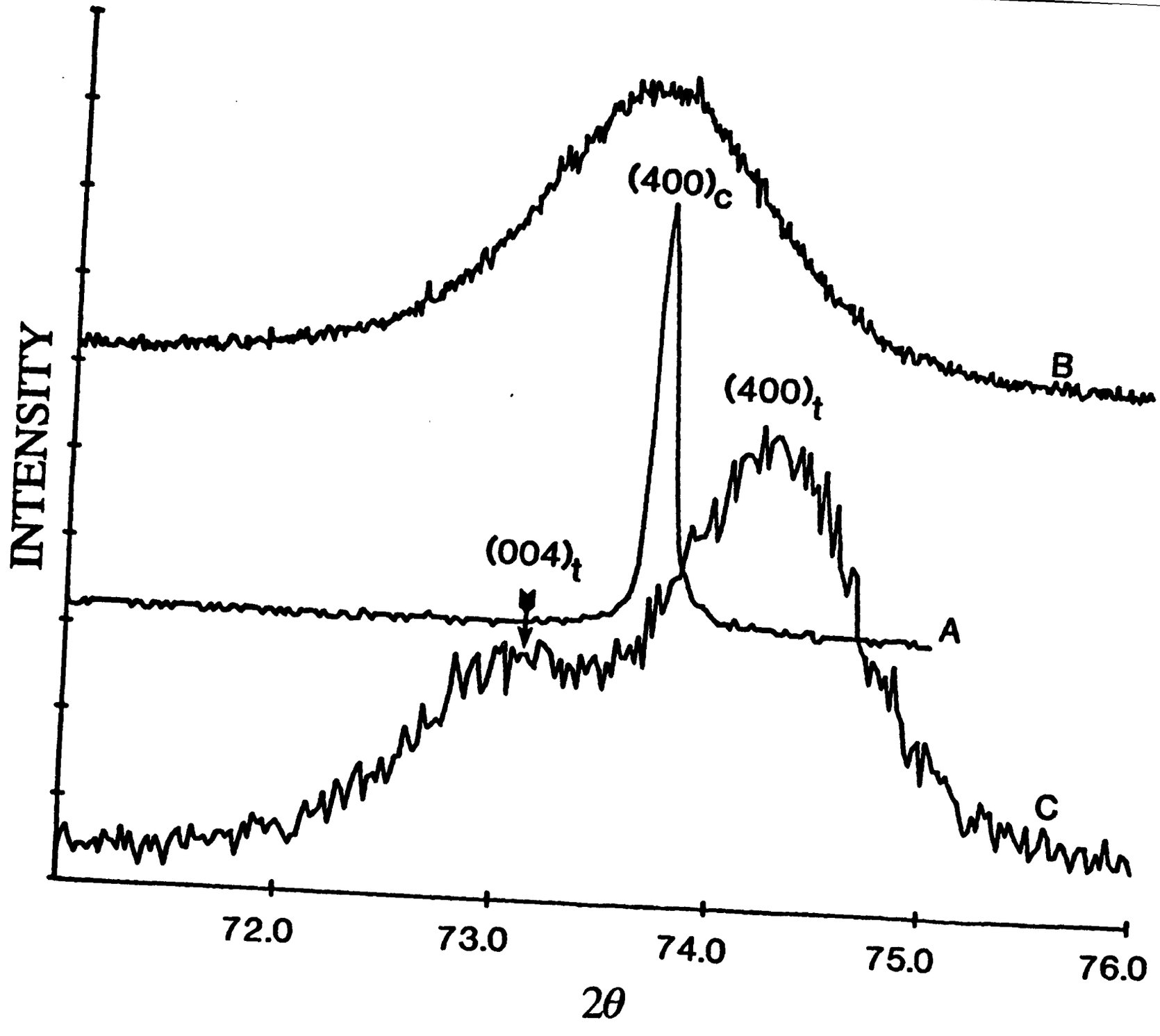

Fig 5

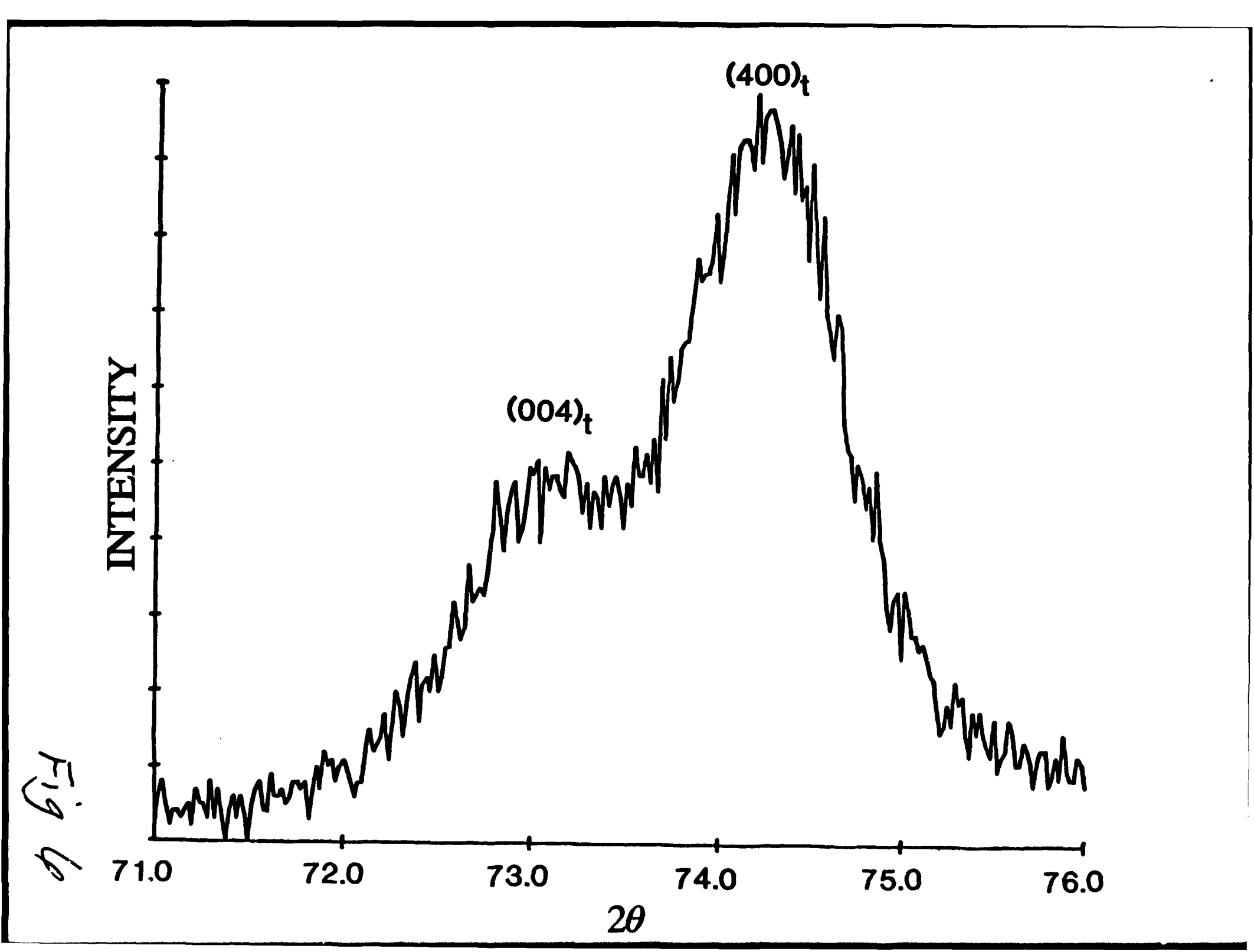

Fig 4

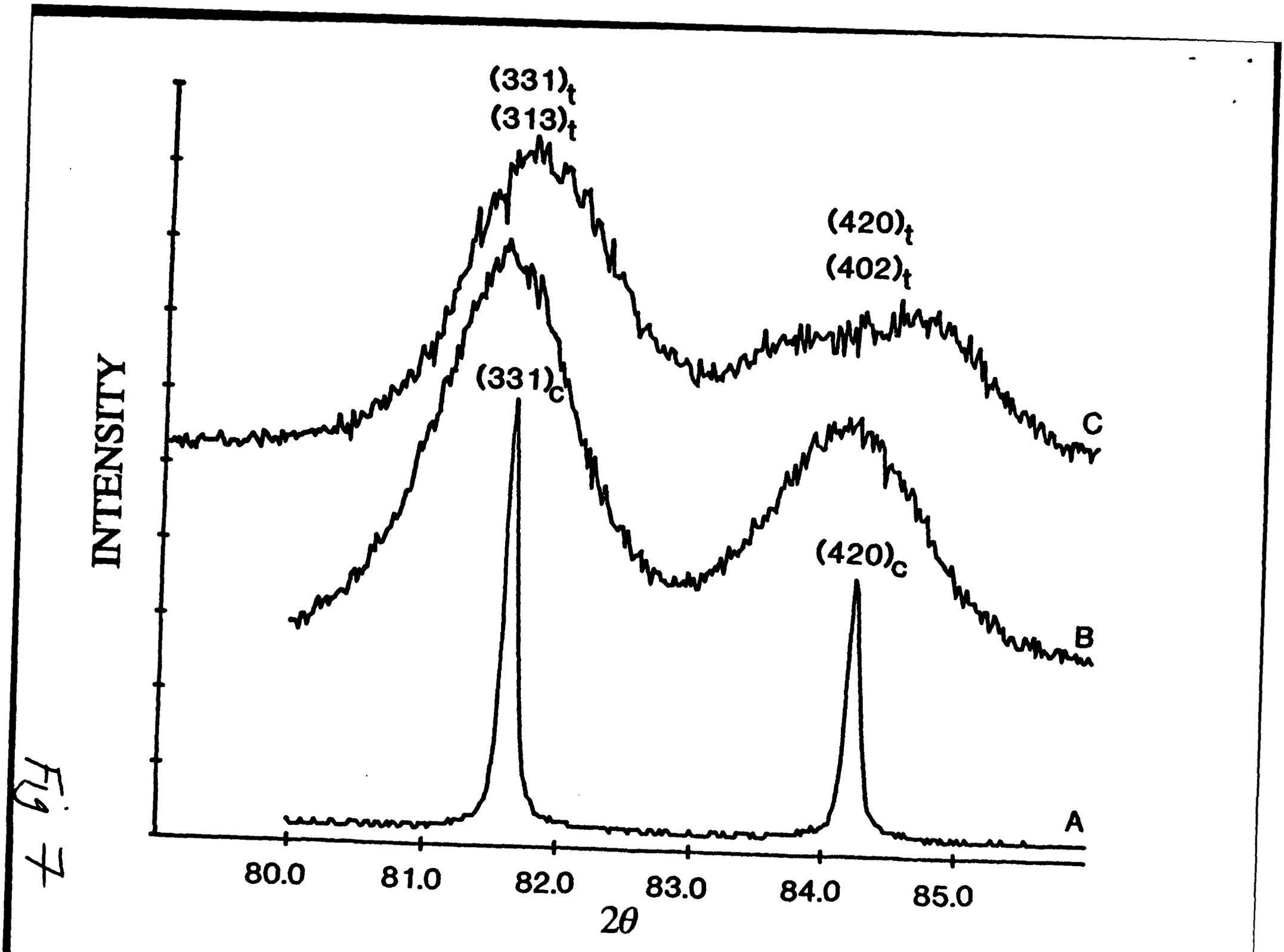
(331)t
(313)t
(420)t
(402)t
(331)c
(420)c
C
B
A
INTENSITY
80.0
81.0
82.0
83.0
84.0
85.0
2θ

Fig 7

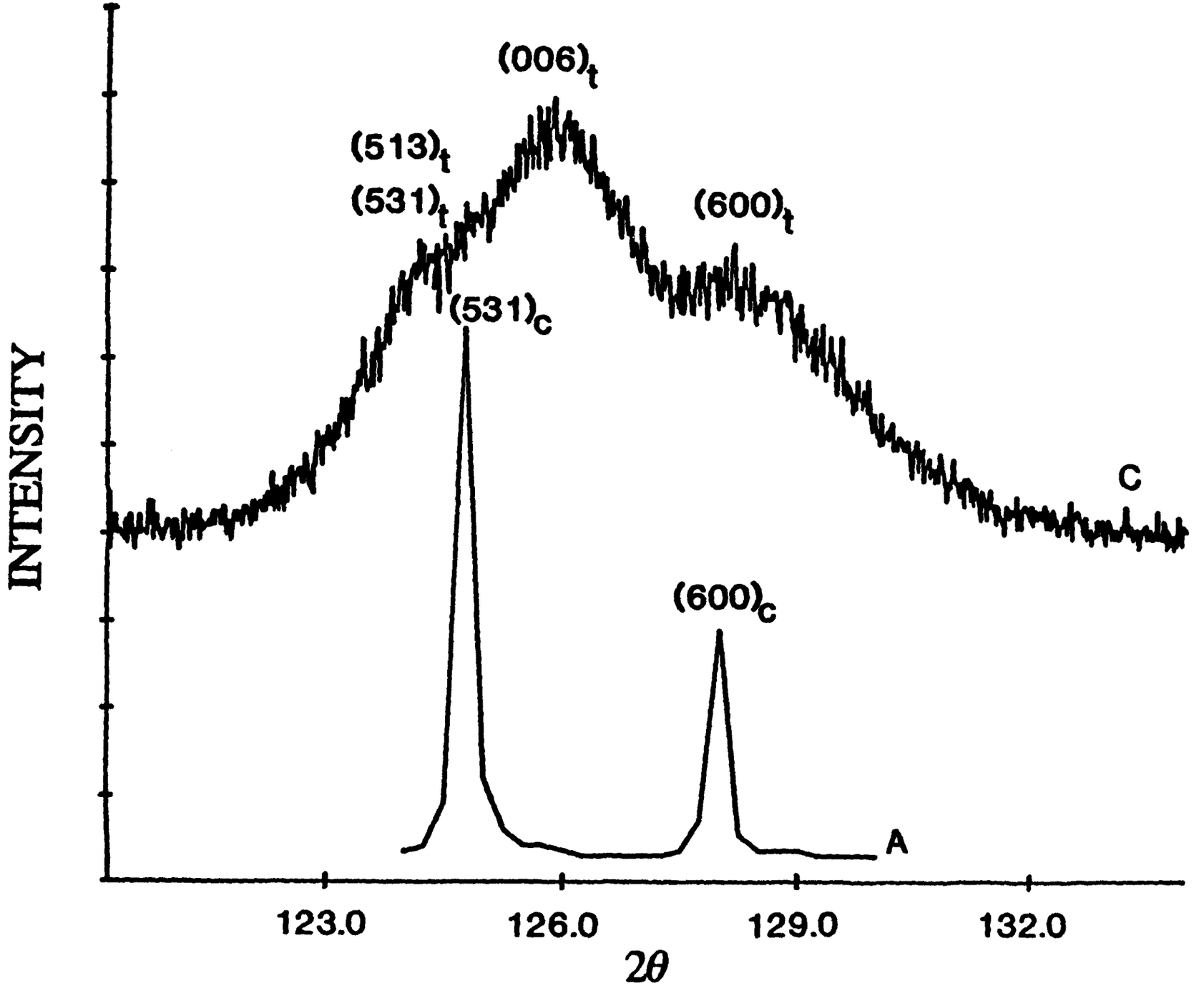
(006)t
(513)t
(531)t
(600)t
(531)c
(600)c
C
A
INTENSITY
123.0
126.0
129.0
132.0
2θ

Fig 8

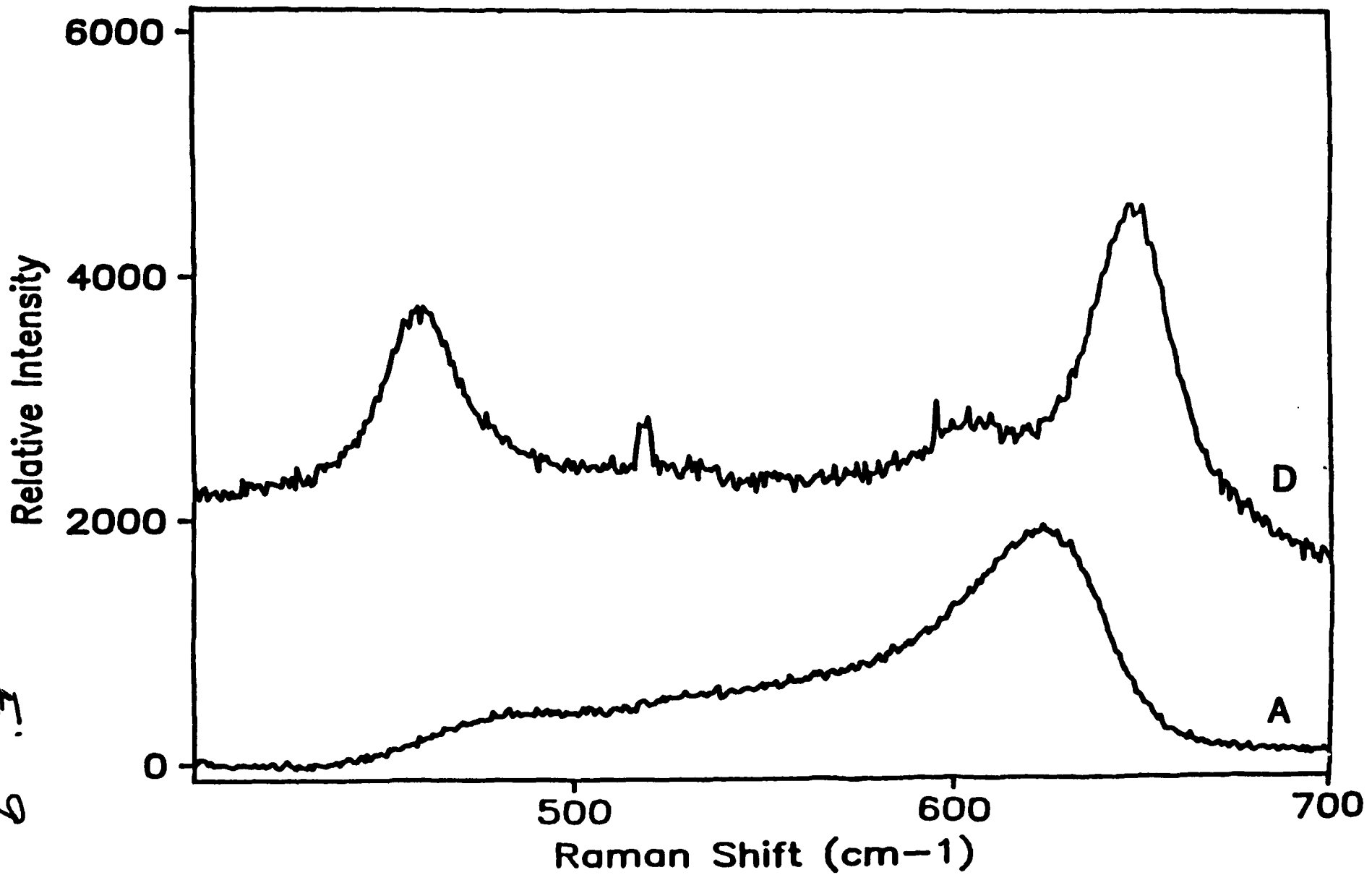
6000
4000
2000
0
Relative Intensity
500
600
700
Raman Shift (cm−1)
D
A

Fig. 9

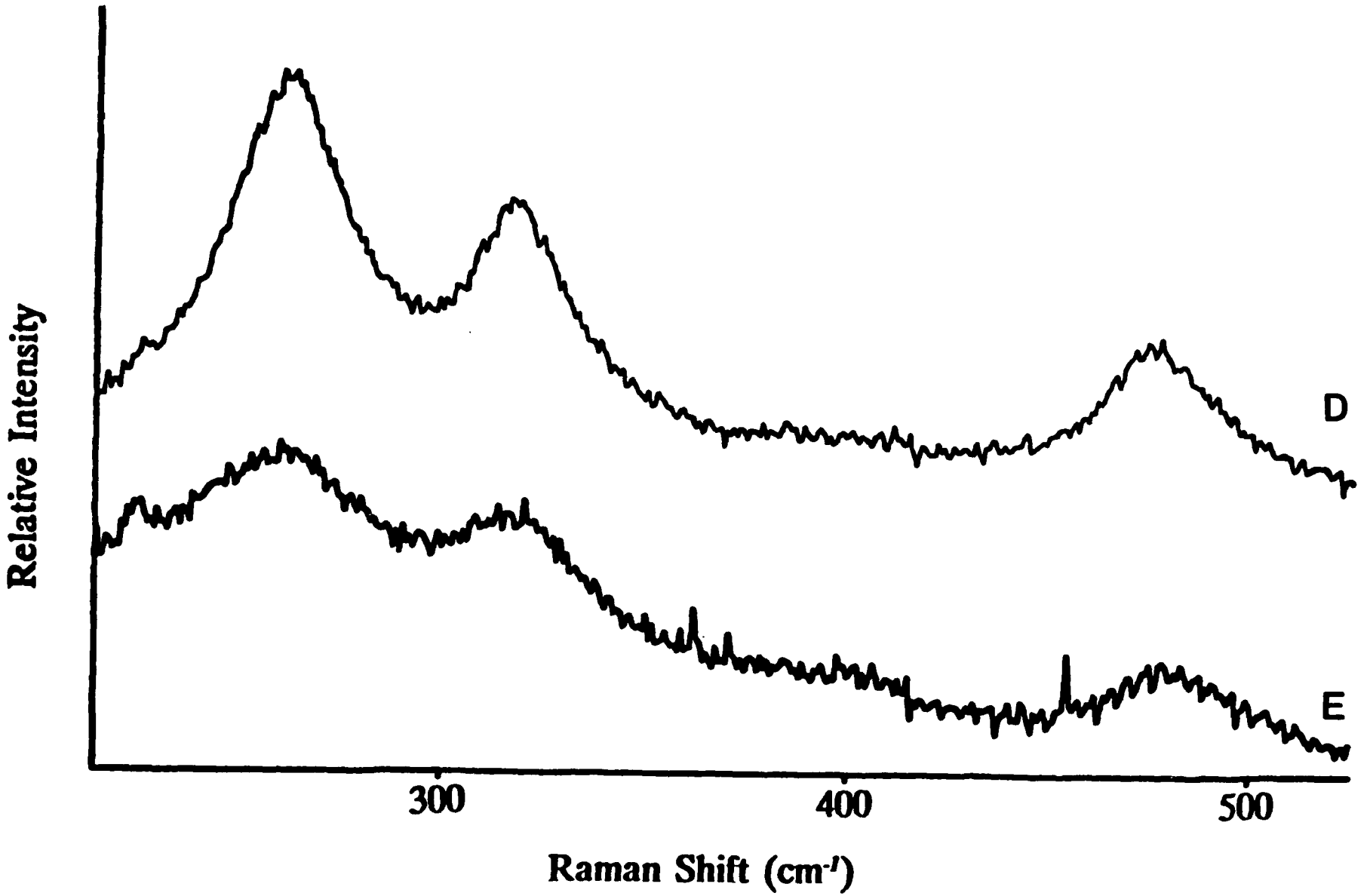

Fig 10

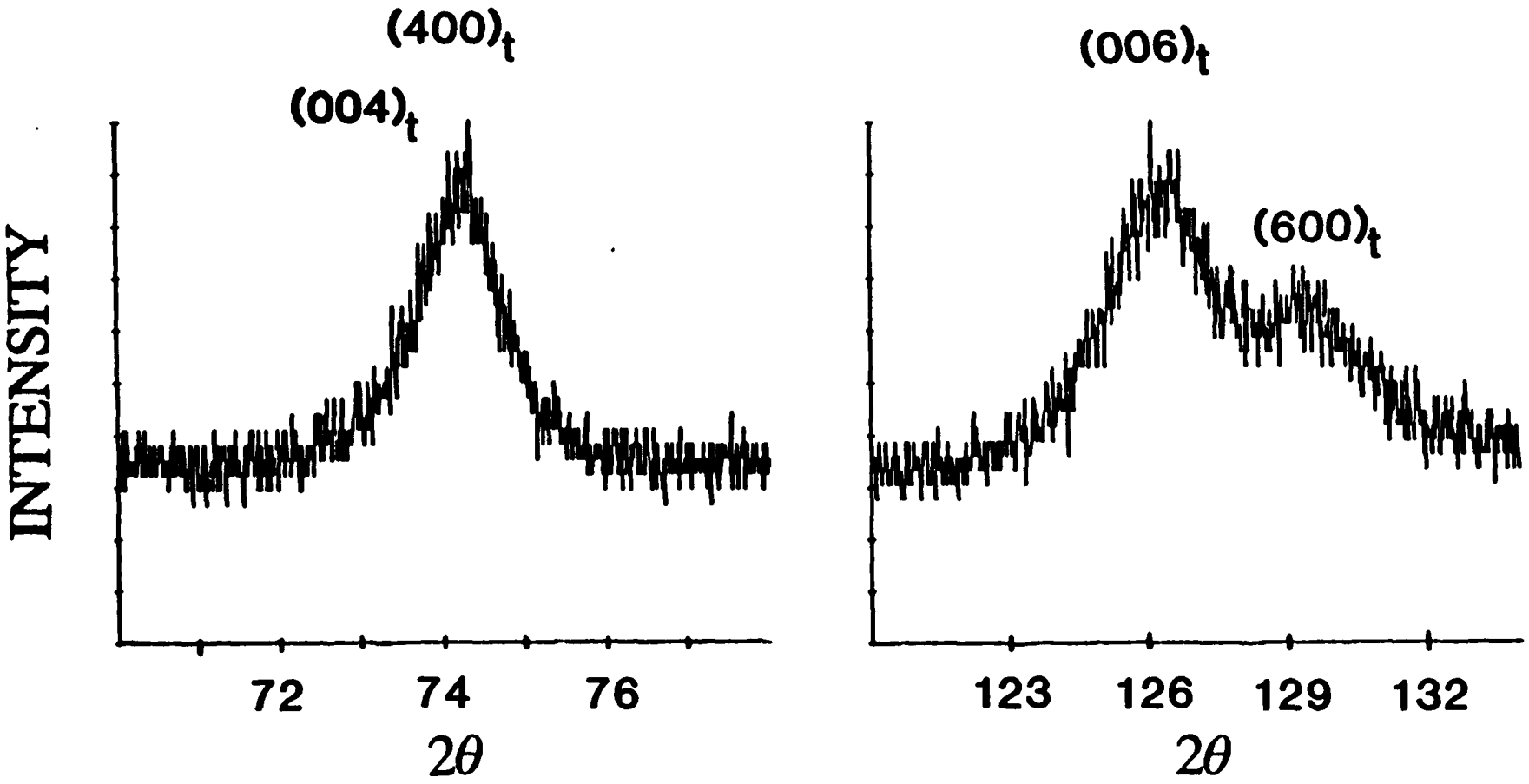

Fig. 11